J. Fluid Mech. (2002), *vol.* 458, *pp.* 269–281.
DOI: 10.1017/S0022112002007929 Printed in the United Kingdom

Integral flow properties of the swash zone and averaging. Part 2. Shoreline boundary conditions for wave-averaged models

By M. BROCCHINI[1] AND G. BELLOTTI[2]

[1]DIAm, Università di Genova, 16145 Genova, Italy

[2]DSIC, Università degli Studi Roma Tre, 00146 Roma, Italy

(Received 24 October 2001 and in revised form 19 December 2001)

Shoreline boundary conditions for nearshore hydrodynamic models are discussed on the basis of the swash zone equations of Brocchini & Peregrine (1996). Swash zone flows are investigated further using the shallow water equations. Results from numerical computations are used to guide approximation to provide more practical boundary conditions for wave-averaged flows. Approximate boundary conditions, valid for small values of the rate of change of the mean water volume in the swash zone, are found which allow explicit computation of a non-zero mean water depth at the mean shoreline. This is computed in terms of the local height of the short waves. Implementation issues are also discussed.

1. Introduction

Nearshore water flows occur over a wide range of time scales. Because of this complexity averaging over the typical period of wind waves (about 10^0–10^1 s) is often introduced. The simplest wave-averaged model, used to compute the wave set-up, is based on the depth-integrated equations for the cross-shore flow motion (1DH). If the flow is non-uniform in the longshore direction two types of models can be employed: 2DH models (based on depth-integrated velocities) and quasi-three-dimensional models.

Although well developed, wave-averaged models use some assumptions which limit their capability of reproducing natural flow conditions. One of the most crucial shortcomings concerns the treatment of the boundary between the wet and dry domains. Since such a boundary is taken as the intersection of the mean water level with the beach face both theoretical and practical problems arise. For instance, the swash zone dynamics is not modelled and flow properties are also defined in regions which should be dry. Moreover, at the mean shoreline the water depth is usually taken to be zero, hence serious computational troubles are faced in prescribing the short-wave (SW) forcing.

We aim to define suitable shoreline boundary conditions (SBCs) for wave-averaged models and analyse in detail SBCs for one-dimensional flow propagation derived from the boundary conditions of Brocchini & Peregrine (1996) (Part 1). We assess validity of the SBCs by means of theoretical and numerical arguments (§ 2) and in § 3 we rewrite them in terms of flow variables used in available wave-averaged models. We simplify them on the basis of numerical solutions of the nonlinear shallow water equations (NSWE) and discuss their features in § 4. Section 5 is devoted to a discussion of issues on the implementation of the SBCs and to some concluding remarks.

2. Evaluation of the chosen SBCs

In Part 1 a detailed analysis of different definitions of mean shoreline revealed that such a mean interface cannot be uniquely defined. It was also shown that flow properties can be unambiguously defined within the wet region if the boundary between wet and dry is taken as the envelope of the rundown positions. Moreover, in view of the major problems in defining conditions at the wet–dry interface for wave-averaged models a set of equations was proposed to be used as SBCs. These were built on the basis of an integral model for the swash zone. The NSWE (equations (2.4) and (4.1) of Part 1), written in terms of the total water depth d and of the depth-independent horizontal velocity $\boldsymbol{u} = (u_x, u_y) = (u, v)$, are integrated over the swash zone width, i.e. between the lower (x_l) and the upper (x_h) boundary of the swash zone. This introduces both local flow properties computed at x_l and integral flow properties such as

$$V = \int_{x_l}^{x_h} d \, \mathrm{d}x, \quad \boldsymbol{P} = \int_{x_l}^{x_h} \boldsymbol{u} d \, \mathrm{d}x, \quad \boldsymbol{\Upsilon} = \int_{x_l}^{x_h} \boldsymbol{\tau} \, \mathrm{d}x, \tag{2.1}$$

which are respectively the volume of water in the swash zone, the momentum of water in the swash zone and the seabed friction force in the swash zone. In the latter the seabed shear stress $\boldsymbol{\tau}$ can be modelled by suitable formulations, one of which is described in the following (see equations (2.7) and (2.8)).

A Reynolds-type decomposition was used for distinguishing between short- and long-wave properties. Hence, a generic property f is decomposed into a long-period ($\langle f \rangle$) and a short-period component as follows:

$$f(\boldsymbol{x}, t) = \begin{cases} \langle f \rangle + \tilde{f}, & \text{if } \boldsymbol{x} \text{ is outside the swash zone,} \\ \langle f \rangle + \hat{f}, & \text{if } \boldsymbol{x} \text{ is inside the swash zone.} \end{cases} \tag{2.2}$$

The decomposition is achieved by assuming the swash motion is almost entirely assigned to SW contributions and that the only long-wave (LW) contribution for a 1DH propagation comes from the motion of the mean shoreline, i.e. of x_l:

$$d = \hat{d}, \quad u = \frac{\mathrm{d}x_l}{\mathrm{d}t} + \hat{u}. \tag{2.3}$$

Use of a different basis for SW and LW properties in the swash zone compared with those outside the swash zone is justified in various ways (see also § 7 of Part 1) which reflect the observation that on many sandy beaches there is a strong difference in the character of the bed in the swash zone compared with the bed just outside the swash zone.

In the case of 1DH flow propagation the two equations which hold at x_l are those obtained respectively from (7.10) and (7.11) of Part 1:

$$\frac{\mathrm{d}x_l}{\mathrm{d}t} = \langle u \rangle + \frac{\langle \tilde{u}\tilde{d} \rangle - \mathrm{d}\langle \hat{V} \rangle / \mathrm{d}t}{\langle d \rangle}, \tag{2.4}$$

$$\frac{\mathrm{d}}{\mathrm{d}t}\left[\langle \hat{P}_x \rangle + \frac{\mathrm{d}x_l}{\mathrm{d}t}\langle \hat{V} \rangle\right] + g\alpha\langle \hat{V} \rangle + \langle \Upsilon_x \rangle = \left[\langle u \rangle - \frac{\mathrm{d}x_l}{\mathrm{d}t}\right]^2 \langle d \rangle + 2\langle \tilde{u}\tilde{d} \rangle \left[\langle u \rangle - \frac{\mathrm{d}x_l}{\mathrm{d}t}\right] + \langle \tilde{u}^2 \rangle \langle d \rangle + \langle \tilde{u}^2 \tilde{d} \rangle + \frac{g}{2}[\langle \tilde{d}^2 \rangle + \langle d \rangle^2] \tag{2.5}$$

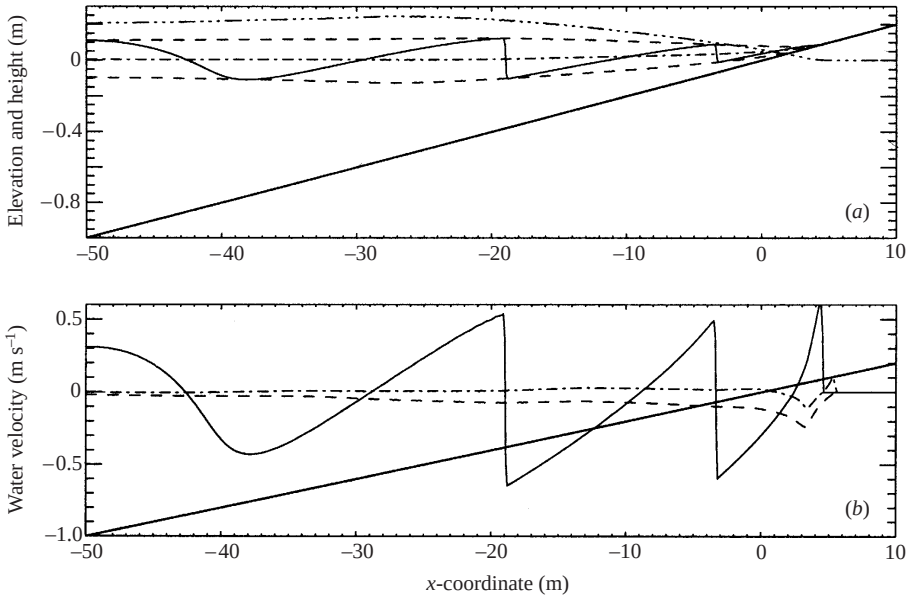

FIGURE 1. An example of solution for the case of $\xi_m = 0.079$ and $f = 0$. (*a*) Instantaneous free surface elevation (solid line) with envelopes of maxima and minima (dashed lines), mean water level (dash-dotted line) and wave height (double-dotted-dashed line). (*b*) Instantaneous velocity (solid line), mean velocity $\langle u \rangle$ (dashed line) and mean velocity $\bar{u}$ (dashed-dotted line) of equation (3.1). In both panels the thick, solid line represents the seabed.

in which α is the beach slope and g the acceleration due to gravity. For more details on the derivation of (2.4) and (2.5) please refer to Part 1.

Since we aim to show the effectiveness of (2.4) and (2.5) in providing SBCs we analyse their behaviour by means of sample solutions of the NSWE. Such equations are obtained by assuming that vertical flow acceleration is small compared with gravity and no dispersive terms are included. Hence solutions for sufficiently steep waves travelling shoreward continually steepen and eventually break. Notwithstanding these approximations the flow motion near the shore over a sloping beach can be successfully modelled by the NSWE (e.g. Kobayashi, Otta & Roy 1987; Watson, Barnes & Peregrine 1994).

We resort to full numerical solutions because analytical solutions, though attractive and useful, are not suited for describing wave breaking conditions which, on the contrary, can be represented by numerical solutions of the NSWE. Moreover, use of a shock-capturing solver which can deal with swash motions (e.g. Watson *et al.* 1994) allows computation of both SW and LW properties in shallow enough water (see figure 1).

In Part 1 examples were only given for a time-independent position of the lower boundary of the swash zone, i.e. for $\mathrm{d}x_l/\mathrm{d}t = 0$. We here extend our analysis to the more complex and practically more important case of an unsteady motion of x_l. Hence the solution must involve at least two wave modes of rather different frequency. We, thus, consider cases in which bichromatic waves and irregular waves (generated on the basis of JONSWAP-type spectra) propagate with breaking of the SWs over beaches of different slopes. The SW mode is characterized either by input length (at the seaward boundary of the domain) and height (L_s, H_s) or by an input 'significant length' (associated with the significant period) and a significant height (L_s^S, H_s^S) and is

superposed on the LW mode of input properties (L_l, H_l). This procedure is particularly suited to numerical computations and allows a strict control of the properties of both SWs and LWs. A second procedure, often used in experimental analysis, could have been employed in which the LW is generated within the considered domain by interaction of the SW. This, however, has one major drawback: the LW height H_l is known with a lesser accuracy than with the former procedure, which is chosen for clarity purposes. Also note that the chosen procedure exactly reproduces what occurs in standard applications of wave-averaged models in which the SW field is represented through one single mode ('representative' or 'significant' wave).

A large number of sample computations has been performed by using typical field conditions but only results of the most representative are reported here. It is well known that the motion of water waves on beaches can be suitably classified in terms of the ratio between the beach slope and the square root of the wave steepness which gives the so called 'Iribarren number' typically used to classify the types of breaking. Our results show (see § 4) that the relative size of contributions to the momentum equation strongly depends both on α and on the input steepness H_s/L_s of the SW. A weaker influence is due to the input LW. This is suitably expressed in terms of the input ratio L_l/L_s, the role of H_l being less important for the cases discussed here. Hence we choose to classify our test conditions in terms of both the 'modified Iribarren number'

$$\xi_m = \frac{\alpha}{\sqrt{(H_s/L_s)(L_l/L_s)}} \tag{2.6}$$

and the dimensionless, scaled friction parameter

$$f = C_f/\alpha \tag{2.7}$$

used to express the seabed shear stress by a Chezy-type formulation such that

$$\langle \Upsilon_x \rangle = \left\langle \int_{x_l}^{x_h} \frac{C_f |u| u}{2} \mathrm{d}x \right\rangle = \left\langle \int_{x_l}^{x_h} \frac{f \alpha |u| u}{2} \mathrm{d}x \right\rangle. \tag{2.8}$$

Although the Chezy friction law is widely used in parameterizing the seabed frictional effects, the debate regarding the size of the frictional coefficients f is still continuing. However, a simple analysis given by Watson *et al.* (1994) reveals a critical value for f such that frictional effects dominate the entire domain of interest. By writing the NSWE in a dimensionless form it is possible to show that the term representing the seabed shear stress is proportional to $f = C_f/\alpha$ and that the critical size for f relates to the beach slope. For $C_f \ll \alpha$ friction is negligible while it has a noticeable effect for $C_f \sim \alpha$.

Experimental investigations show that the dimensionless friction coefficient C_f ranges between 0.01 and 0.04 (e.g. Puleo & Holland 2001). Moreover experiments with breaking waves show that for very mildly sloping beaches ($\alpha \leqslant 0.01$) breaking is intermittent and solutions of the NSWE solver may not be adequate, hence we used $0.02 \leqslant \alpha \leqslant 0.1$.

For the test conditions analysed $0.02 \leqslant \xi_m \leqslant 0.40$ and $0 \leqslant f \leqslant 1$. The smallest values of ξ_m characterize steep SWs and relatively long LWs while the largest values of ξ_m pertain to less steep SWs superposed on relatively short LWs. Both ξ_m and f vary over a range which is representative of typical wave conditions over most natural beaches.

Results of computations illustrate a number of features of the chosen equations and support the validity of the analytical derivation given in Part 1. We can reproduce

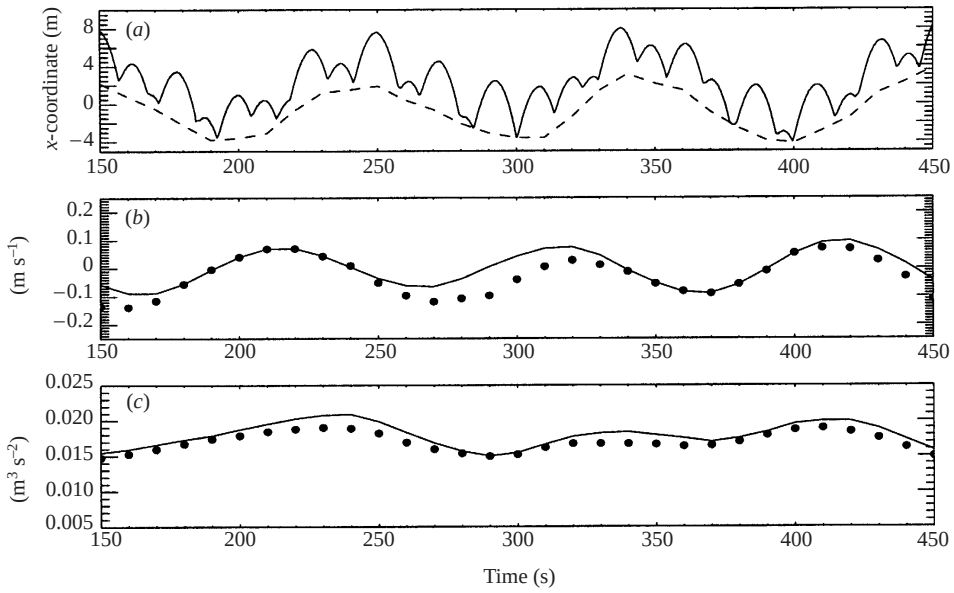

FIGURE 2. Results of the validation procedure for the case of irregular waves of $\xi_m = 0.079$ and $f = 0$. (*a*) Instantaneous (solid line) and mean (dashed line) shorelines. (*b*, *c*) Left-hand side (—) and right-hand side (• • •) of equations (2.4) and (2.5) respectively.

the position of the instantaneous shoreline and the motion of the seaward limit of the swash zone whose envelope gives the chosen mean shoreline (see figure 2*a*). Moreover, comparison of the left-hand side with the right-hand side of the model equations (see figure 2*b*, *c*) shows it is possible to predict both the motion of x_l and the water depth at x_l once the SW properties are known.

Although a good agreement exists between signals representing the left-hand side and the right-hand side of equations (2.4) and (2.5), matching is not perfect as it should be for conservation equations. Disagreement is due to two practical reasons. First, the 'operative definition' of the lower boundary of the swash zone x_l brings with it some uncertainties caused by computing the envelope of the rundown positions. The procedure we used is similar to that described in Shah & Kamphuis (1996) which involves low-pass filtering of the instantaneous shoreline position. Such an operation introduces uncertainties which become smaller and smaller on decreasing the number of modes that make up the signal of the instantaneous shoreline. Comparisons equivalent to that proposed in figure 2 but employing bichromatic waves give almost-perfect visual matching. However, even in this case the matching is not exact because of numerical errors caused by the accuracy of the numerical method and of the discretization used.

Notice that for these tests SW properties are those derived from the computations but to use the equations as a predictive tool we must prescribe them through a suitable theory. We discuss this in § 5.

3. Features of the SBCs

Before discussing the features of the SBCs (2.4) and (2.5) we write them in a form consistent with the flow description employed in available wave-averaged models. Different definitions of mean flow variables are used in the literature dealing with

wave-averaged models. In models like those of Özkan-Haller & Kirby (1997) and of Van Dongeren & Svendsen (2000) the mean flow velocity, which we label as $\bar{u}$ to distinguish it from the mean velocity $\langle u\rangle$ used in Part 1, is defined as the time-average of the total mass flux divided by the mean depth. On the other hand, there is no ambiguity in the definition of the mean water depth and $\bar{d}$ (the overbar is only used for uniformity of notation) coincides with $\langle d\rangle$:

$$\bar{d} = \langle d\rangle, \quad \bar{u} = \langle u\rangle + \frac{\langle \tilde{u}\tilde{d}\rangle}{\langle d\rangle}. \tag{3.1}$$

Moreover, it is common practice to use the following nonlinear SW variables:

$$\langle \tilde{Q}\rangle = \langle \tilde{u}\tilde{d}\rangle = \text{SW mass flux}, \tag{3.2a}$$

$$\langle \tilde{S}\rangle = \langle \tilde{u}^2\rangle \bar{d} + \langle \tilde{u}^2\tilde{d}\rangle + \frac{g}{2}\langle \tilde{d}^2\rangle = \text{SW momentum flux or 'radiation stress'}. \tag{3.2b}$$

Hence, substitution of (3.1) and (3.2) into both (2.4) and (2.5) gives the desired form of the SBCs:

$$\frac{\mathrm{d}x_l}{\mathrm{d}t} = \bar{u} - \frac{1}{\bar{d}}\frac{\mathrm{d}\langle \hat{V}\rangle}{\mathrm{d}t}, \tag{3.3}$$

$$\frac{\mathrm{d}}{\mathrm{d}t}\left[\langle \hat{P}_x\rangle + \frac{\mathrm{d}x_l}{\mathrm{d}t}\langle \hat{V}\rangle\right] + g\alpha\langle \hat{V}\rangle + \langle \Upsilon_x\rangle = \left[\bar{u}^2 + \left(\frac{\mathrm{d}x_l}{\mathrm{d}t}\right)^2\right]\bar{d} - 2\bar{u}\bar{d}\,\frac{\mathrm{d}x_l}{\mathrm{d}t} + \frac{1}{2}g\bar{d}^2 - \frac{\langle \tilde{Q}\rangle}{\bar{d}} + \langle \tilde{S}\rangle. \tag{3.4}$$

A third equation is required for completely solving for the mean flow, i.e. determining both the motion of x_l and the values of both $\bar{d}(x_l)$ and $\bar{u}(x_l)$. This must provide some information on what is happening inside the computational domain. Such information is carried by the positive (incoming) Riemann variable $R_+ = \bar{u} + 2\sqrt{g\bar{d}}$ which propagates from the interior towards the shoreline along positive characteristics of the NSWE for the mean flow (e.g. Özkan-Haller & Kirby 1997):

$$\frac{\mathrm{d}R_+}{\mathrm{d}t} = -g\alpha - \frac{1}{\bar{d}}\frac{\mathrm{d}\langle \tilde{S}\rangle}{\mathrm{d}x} \quad \text{along} \quad \frac{\mathrm{d}x}{\mathrm{d}t} = \bar{u} + \sqrt{g\bar{d}}. \tag{3.5}$$

Now the three equations (3.3), (3.4) and $R_+ = \bar{u} + 2\sqrt{g\bar{d}}$ can be solved for x_l, $\bar{d}$ and $\bar{u}$ once R_+ is known at x_l from (3.5). They can also be simplified on the basis of the following analyses which aims at obtaining one first set of SBCs which can be considered as exact within the approximation of wave-averaged shallow water flows and for beaches of natural slope.

Therefore we restrict our analysis to the case of beach slopes large enough that the acceleration of the mean shoreline is negligible. Thus for $\alpha \gg (\mathrm{d}^2x_l/\mathrm{d}t^2)/g$ we can neglect $\mathrm{d}^2x_l/\mathrm{d}t^2$ with respect to $g\alpha$ on the left-hand side of (3.4). Computations suggest a maximum acceleration of the mean shoreline of about $0.001\,\mathrm{m\,s^{-2}}$ which is about ten times larger than measured accelerations in the field (Guza & Thornton 1985). For typical wave conditions this means that we restrict our attention to beaches of slope larger than about 1 : 1000 which is almost always the case for natural beaches. A simple manipulation gives the following form of the SBCs:

$$\bar{u} = R_+ - 2\sqrt{g\bar{d}}, \tag{3.6a}$$

$$\frac{\mathrm{d}x_l}{\mathrm{d}t} = R_+ - \frac{2\sqrt{g\bar{d}^3} + \mathrm{d}\langle \hat{V}\rangle/\mathrm{d}t}{\bar{d}}, \tag{3.6b}$$

$$\underbrace{g\bar{d}^3}_{\text{(I)}} + \underbrace{4\sqrt{g}\frac{\mathrm{d}\langle\hat{V}\rangle}{\mathrm{d}t}\bar{d}^{3/2}}_{\text{(II)}} - \underbrace{2\left[\frac{\mathrm{d}\langle\hat{P}_x\rangle}{\mathrm{d}t} + g\alpha\langle\hat{V}\rangle + \langle\Upsilon_x\rangle + R_+\frac{\mathrm{d}\langle\hat{V}\rangle}{\mathrm{d}t} - \langle\tilde{S}\rangle\right]\bar{d}}_{\text{(III)}}$$

$$+ \underbrace{4\left[\frac{\mathrm{d}\langle\hat{V}\rangle}{\mathrm{d}t}\right]^2}_{\text{(IV)}} - 2\langle\tilde{Q}\rangle^2 = 0. \quad (3.6c)$$

The terms containing the four different powers of $\bar{d}$ in (3.6*c*) have been labelled with Roman capital figures for ease of reference in the following analyses.

Since SW properties in principle depend on LW characteristics, equation (3.6*c*) cannot be solved directly. However the above set of coupled equations can be solved by an iterative procedure: a trial solution of (3.6*c*) can be substituted into (3.6*a*) and (3.6*b*) to give an approximate value of both $\mathrm{d}x_l/\mathrm{d}t$ and $\bar{u}$. A similar iterative procedure is sometimes used in wave-averaging solvers and is found to converge in few iterations (e.g. Haas, Svendsen & Haller 1998). However, a simpler solution strategy is most often used which is based on the assumption of a weak dependence of SW properties on $\bar{d}$ and $\bar{u}$. In that case (3.6*c*) is an algebraic equation in $\bar{d}$ and an analytical solution for $\bar{d}$ can be found. This is the approach we use in the following, having in mind that an iterative procedure can be easily implemented once a good trial value for $\bar{d}$ is found.

Once a method is found to compute the positive Riemann variable at x_l it is possible to implement conditions (3.6) into available models like SHORECIRC (Van Dongeren & Svendsen 2000). However, we aim at understanding properties of conditions (3.6) and look for an approximate version of such conditions which can lead to an analytical solution of the problem. We start by analysing the following two special cases.

(i) *The motion of a 'rigid wall'*

This case is characterized by no water in the swash zone (i.e. $\langle\hat{V}\rangle = 0$, $\langle\hat{P}_x\rangle = 0$, $\langle\Upsilon_x\rangle = 0$) and simplifies to

$$\frac{\mathrm{d}x_l}{\mathrm{d}t} = \bar{u} = R_+ - 2\sqrt{g\bar{d}}, \quad (3.7a)$$

$$g\bar{d}^3 + 2\langle\tilde{S}\rangle\bar{d} - 2\langle\tilde{Q}\rangle^2 = 0. \quad (3.7b)$$

These conditions are those of a rigid wall moving with velocity $\bar{u}$ (equation (3.7*a*)) where the water depth can change due to the change in the SW forcings $\langle\tilde{Q}\rangle$ and $\langle\tilde{S}\rangle$ of equation (3.2).

This type of condition was discussed in § 7 of Part 1 in which an indication was also given of the treatment of SWs at the wall. SWs are perfectly reflected so that, in the assumption that for known mean flow properties they can be suitably described in terms of only the wave height and period, the following holds:

$$H_{out} = H_{in}, \quad \frac{1}{T_{out}} = \frac{1}{T_{in}} - \frac{2\bar{u}}{L_{in}}, \quad (3.8)$$

in which the subscripts *in* and *out* label the properties of SWs respectively incident and reflected at the wall.

(ii) *Steady-state conditions*
If steady-state conditions are assumed equation (3.6*c*) simplifies to

$$g\bar{d}^3 - 2[g\alpha\langle\hat{V}\rangle + \langle\Upsilon_x\rangle - \langle\tilde{S}\rangle]\bar{d} - 2\langle\tilde{Q}\rangle^2 = 0 \tag{3.9}$$

and gives a depth of equilibrium at x_l for given SW properties ($\langle\hat{V}\rangle$, $\langle\tilde{Q}\rangle$, $\langle\tilde{S}\rangle$ and $\langle\Upsilon_x\rangle$).

It is clear that cases (i) and (ii) are only useful for illustrative purposes. A more general and useful case is described in the next section in which an approximate version of equation (3.6*c*) is derived on the basis of results of numerical solutions of the NSWE rather than on the basis of *a prioristic* assumptions. Hence, a large number of solutions is used to assess the relative size of each contribution to (3.6*c*), which is consequently simplified (see § 4) by retaining the leading contributions, i.e. those terms which balance in size within the equation (terms of one order of magnitude smaller than the leading terms, in practice less than about 10% smaller, are considered as negligible). The aim is to show that such a simplified problem admits an analytical solution which models well and interprets the results of full numerical solutions and which allows a very simple formulation of the SBCs (see § 5).

4. Some approximate SBCs

These are the SBCs we suggest implementing in available wave-averaged models. They are a slightly simplified version of (3.6) and allow both for the mean shoreline to move (i.e. $\mathrm{d}x_l/\mathrm{d}t \neq 0$) and for SW flows of mass and momentum to take place across the boundary. The major simplification concerns the rate of change of the mean water volume in the swash zone ($\mathrm{d}\langle\hat{V}\rangle/\mathrm{d}t$ appears in various terms of both (3.6*b*) and (3.6*c*)). This is found to contribute negligibly to the momentum balance expressed by equation (3.6*c*).

We have evaluated the size of each contribution to the SBCs on the basis of sample solutions. Analysis of the results reveals that these can be grouped into three classes depending on the value of ξ_m. In each class the values of the computed results are very similar for all properties, their variation being between 10% and 20% of the values reported in table 1. As already mentioned in § 2 results are most sensitive to changes of the slope of the SW, less to changes of the ratio L_l/L_s and of H_l, hence the use of ξ_m of equation (2.6).

The first class (class 'A') is such that $\xi_m < 0.054$ and approximately corresponds to that of 'spilling breakers'. These waves start breaking quite far from the shoreline and, within the NSWE scheme, are characterized by intense energy dissipation which results in reduced swash zone amplitudes. This causes some numerical problems. In fact, in order to adequately resolve swash zone flows, a quite fine numerical discretization was required. If for standard NSWE computations the wavelength of SWs is typically resolved with about 20 to 50 computational points, we had to use up to 450 computational points per wavelength for the tests reported here.

The intermediate class 'B' is characterized by $0.054 \leqslant \xi_m \leqslant 0.150$ and includes waves breaking in the form of 'plungers'. For $\xi_m > 0.150$ the SWs break very close to the shoreline (class 'C').

One first important result is that regardless of the values of the wave parameters, of α and f, the ratio $|\mathrm{d}\langle\hat{V}\rangle/\mathrm{d}t|/|\bar{u}\bar{d}|$ ranges between 0.1 and 0.5. Thus the $\mathrm{d}\langle\hat{V}\rangle/\mathrm{d}t$ contribution to the right-hand side of both (3.3) and (3.6*b*) must be retained in the equation used to prescribe the motion of the shoreline.

Moreover, $\mathrm{d}\langle\hat{P}_x\rangle/\mathrm{d}t$ contributes less than 5% to the coefficient of term (III) of

Wave type	f	Class	$\frac{[4(\mathrm{d}\hat{V}/\mathrm{d}t)^2]}{(2\langle\tilde{Q}\rangle^2)}$	$\frac{(\mathrm{I})}{(\mathrm{IV})}$	$\frac{(\mathrm{II})}{(\mathrm{IV})}$	$\frac{(\mathrm{III})}{(\mathrm{IV})}$	$\frac{R_+\mathrm{d}\hat{V}/\mathrm{d}t}{(\mathrm{III})}$
Bichromatic	0	A	0.0025	2.42	0.08	1.18	0.08
Bichromatic	0	B	0.0013	0.60	0.05	0.48	0.03
Bichromatic	0	C	0.0001	0.59	0.01	0.63	0.01
Bichromatic	0.5	A	0.0044	4.28	0.06	4.62	0.04
Bichromatic	0.5	B	0.0031	2.93	0.05	2.35	0.06
Bichromatic	0.5	C	0.0018	2.76	0.04	1.88	0.06
Bichromatic	1	A	0.0051	6.97	0.22	9.13	0.04
Bichromatic	1	B	0.0043	5.25	0.19	5.15	0.06
Bichromatic	1	C	0.0040	4.67	0.15	4.42	0.06
Irregular	0	A	0.0520	46.20	2.20	52.00	0.11
Irregular	0	B	0.0470	33.00	2.00	35.90	0.12
Irregular	0	C	0.0780	49.10	3.26	51.20	0.13

TABLE 1. Computed results.

equation (3.6*c*) for all the cases considered and, therefore, is neglected. Notice that for perfectly symmetric swashes (with respect to the time of maximum runup) not only is $\mathrm{d}\langle\hat{P}_x\rangle/\mathrm{d}t$ small but it can be shown that $\langle\hat{P}_x\rangle$ identically vanishes (see for example the results computed by means of the Carrier & Greenspan (1958) solution in Part 1). However, for the cases considered here, in which breaking and seabed friction determine asymmetric swashes, numerical results show that $\langle\hat{P}_x\rangle$ does not vanish although its time-derivative is small.

Other important computed results which synthetically describe the analysed flow conditions are summarized in table 1. In each column the largest value of ratios between the size (absolute value of the mean over each wave cycle) of contributions to (3.6*b*) and (3.6*c*) is shown.

We gauge each contribution to (3.6*c*) by the value of the term (IV) which does not contain the unknown $\bar{d}$. The fourth column of table 1 shows that for all flow conditions this almost (i.e. with discrepancies of less than 1%) coincides with $2\langle\tilde{Q}\rangle^2$. It is also clear that the contribution of (II) is at least ten times smaller than the leading terms for all the test conditions considered (see sixth column of table 1) and, as already mentioned, is taken as negligible. Moreover, we can also neglect the $R_+\mathrm{d}\langle\hat{V}\rangle/\mathrm{d}t$ contribution to the coefficient of $\bar{d}$ appearing in (3.6*c*) (see eighth column of table 1).

Analysis of the table also reveals the important role of the friction contribution. This is such as to modify the balance among the various terms of (3.6*c*). For $f = 0$ the balance is such that only (II) can be neglected, the other three terms being of the same size, while for $f = 0.5$ the term (IV) becomes smaller (about one fourth) than both (I) and (III). Finally, for $f = 1$ it would be possible also to neglect (IV) the approximate balance being between (I) and (III). Similar findings are valid for irregular waves even in the case of $f = 0$. These results are useful as a guide to simplifying (3.6*c*) while retaining both unsteadiness of the motion of x_l and allowing for flows across the boundary. Retaining (IV) even for $f \geqslant 0.5$ and irregular waves:

$$\frac{\mathrm{d}x_l}{\mathrm{d}t} = \bar{u} = R_+ - \frac{2\sqrt{g\bar{d}^3} + \mathrm{d}\langle\hat{V}\rangle/\mathrm{d}t}{\bar{d}}, \tag{4.1a}$$

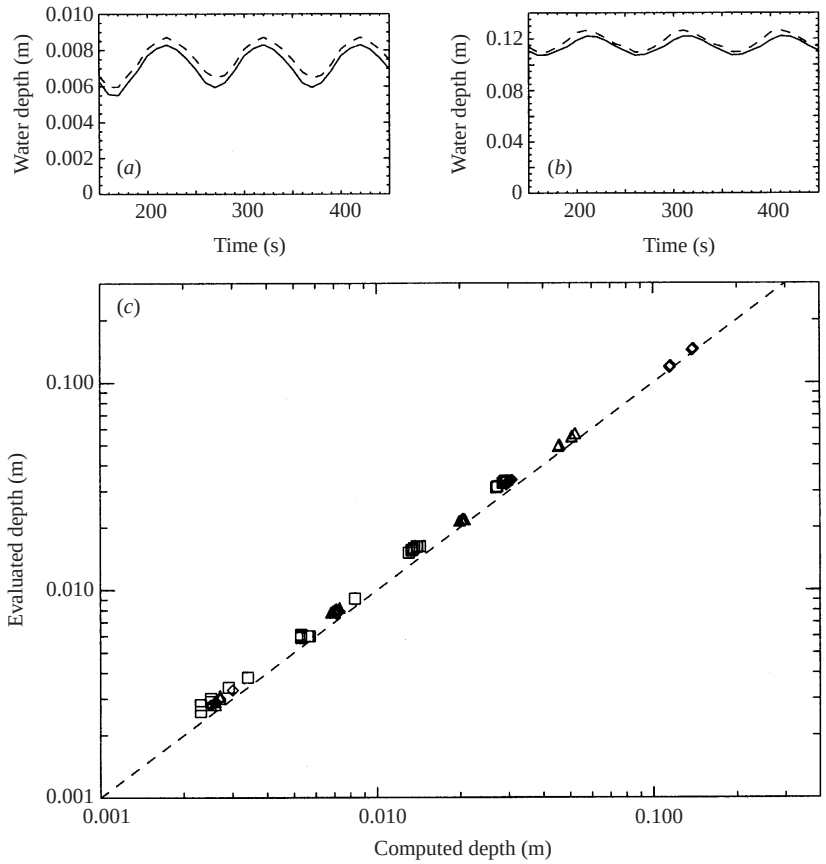

FIGURE 3. (a, b) Comparison of the time series of $\bar{d}_{comp}$ (solid line) and $\bar{d}_{eval}$ (dashed line) for the case $\xi_m = 0.079, f = 0$ (a) and $\xi_m = 0.250, f = 0$ (b). (c) Mean values of $\bar{d}_{comp}$ vs. $\bar{d}_{eval}$ for the cases $f = 0$ (diamonds), $f = 0.5$ (triangles) and $f = 1$ squares. The dashed line gives a reference for the case of perfect matching.

$$g\bar{d}^3 - 2[g\alpha\langle\hat{V}\rangle + \langle\Upsilon_x\rangle - \langle\tilde{S}\rangle]\bar{d} - 2\langle\tilde{Q}\rangle^2 = 0. \tag{4.1b}$$

In this case the coefficients of equation (4.1b) are only a function of the SW motion. One first important consequence of the above is that (4.1b) is unaffected by the positive Riemann invariant and the depth at the mean shoreline is only imposed by the SW properties. This is in good agreement with the fundamental assumption (see also Part 1) that the swash zone motion is entirely assigned to SW contributions and that LWs only force the motion of the mean shoreline. One practical implication is that standard techniques can be used to model the motion of the mean shoreline (e.g. Bellotti & Brocchini 2001) but a non-zero depth is attained at the mean shoreline which depends on the local SW conditions and is found by solving (4.1b). Also, this finding is not surprising in view of the analysis performed in Part 1 on the characteristics of mean shorelines. For example, figure 8 of Part 1 shows the dependence on the wave amplitude of the mean water depth at the location given by the phase-averaged waterline. However, that result is specific to the analytical solution of Carrier & Greenspan (1958) while the result found here holds at x_l and is more general, also covering the case of breaking waves.

Results of the comparison between the value of $\bar{d}$ determined from the numerical

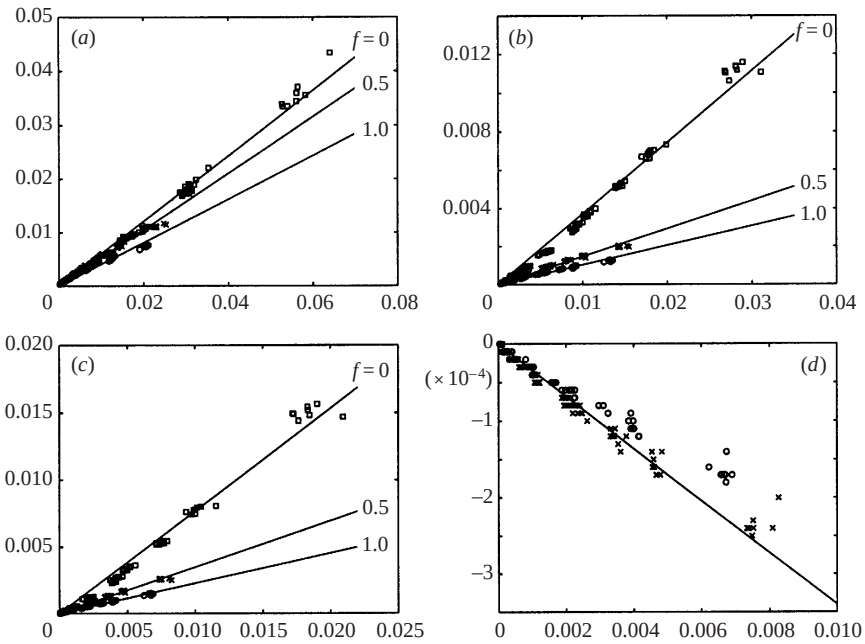

FIGURE 4. Fitting of SW properties. (*a*)–(*d*) The first four properties of equation (5.1): $\langle \hat{V} \rangle$, $\langle \tilde{Q} \rangle$, $\langle \tilde{S} \rangle$ and $\langle \Upsilon_x \rangle$ respectively.

solution of the NSWE ($\bar{d}_{comp}$) and that evaluated by equation (4.1*b*) ($\bar{d}_{eval}$) are reported on figure 3. Panels (*a*) and (*b*) show the comparison of the time series of the functions for two specific tests while panel (*c*) collects the mean values of both signals for all the cases considered here. The latter plot shows that $\bar{d}_{eval}$ overpredicts $\bar{d}_{comp}$ (symbols are above the straight line of reference) by about 5%–15%; however a good overall agreement exists between the two data sets. The overprediction weakly depends on f and an improving agreement is achieved for increasing values of $\bar{d}$, i.e. for increasing ξ_m.

5. Implementation of the SBCs

As already mentioned, in principle conditions (3.6) could be directly implemented in available solvers but we prefer to discuss use of the simplified conditions (4.1) as they are more amenable to analytical treatment and more suited for illustration purposes.

The main problem in implementing SBCs is to suitably predict $\bar{d}(x_l)$ on the basis of local (computed at x_l) SW conditions. This requires a good prescription of the SW coefficients of equation (4.1) in terms of the local wave parameters (H, T), of α and f.

Dimensional arguments and analytical results based on the Carrier & Greenspan (1958) solution (e.g. Mei 1989, pp. 524–527) and the Shen & Meyer solution (e.g. Peregrine & Williams 2001) suggest that the swash zone width scales with H/α while, in very shallow water, the most suitable scale for the water depth is H. Hence according to (2.1*a*) $\langle \hat{V} \rangle$ scales with H^2/α. Definition (3.2*a*) suggests that $\langle \tilde{Q} \rangle$ scales with the product of the scale for the onshore velocity of the SW (in shallow water $\sqrt{gH}$) times the scale for the fluctuation of the water depth (H). In shallow water the

radiation stress $\langle\tilde{S}\rangle$ is suitably scaled with gH^2 and it is easy to show that $\langle\Upsilon_x\rangle$ scales with fgH^2, hence

$$\langle\hat{V}\rangle = C_V\frac{H^2}{\alpha},\ \langle\tilde{Q}\rangle = C_Q\sqrt{gH^3},\ \langle\tilde{S}\rangle = C_S gH^2,\ \langle\Upsilon_x\rangle = C_\Upsilon gH^2,\ \frac{\mathrm{d}\langle\hat{V}\rangle}{\mathrm{d}t} = \frac{2C_V H}{\alpha}\frac{\mathrm{d}H}{\mathrm{d}t}, \tag{5.1}$$

with

$$C_V = 0.615 - 0.201f,\ C_Q = 0.356 - 0.273\sqrt{f},\ C_S = 0.792 - 0.574\sqrt{f},\ C_\Upsilon = -0.034f. \tag{5.2}$$

These values, obtained from fitting (with a regression coefficient ranging between 0.94 and 0.99 as shown in figure 4) a large number of solutions, give an excellent representation of the SW properties of (5.1) over a wide range of H, T, α and f. Hence, the coefficients of (3.6*b*) can be directly referred to the local height of the SWs by substitution of (5.1), into (4.1*b*):

$$\bar{d}^3 - 2(C_V + C_\Upsilon - C_S)H^2\bar{d} - 2C_Q^2H^3 = 0. \tag{5.3}$$

This equation is amenable to simple, analytical solution (see Abramowitz & Stegun 1964). First, the condition

$$[C_Q^4 - \tfrac{8}{27}(C_V + C_\Upsilon - C_S)^3]H^6 > 0 \tag{5.4}$$

valid for $f < 0.5$, states that equation (5.3) admits one real and two complex conjugate roots. The real root is then computed to give

$$\bar{d} = [(1+F)^{1/3} + (1-F)^{1/3}]C_Q^{2/3}H \quad \text{where} \quad F = \sqrt{1 - \frac{8(C_V + C_\Upsilon - C_S)^3}{27C_Q^4}}. \tag{5.5}$$

Substitution for C_V, C_Q, C_S and C_Υ gives the desired solution:

$$0.45H \leqslant \bar{d} \leqslant 0.55H \quad \text{for} \quad 0 \leqslant f \leqslant 0.5. \tag{5.6}$$

This almost coincides with the range $0.48H \leqslant \bar{d} \leqslant 0.53H$ derived from the fully numerical solution of the NSWE, demonstrating again both the validity of the chosen SBCs and of the chosen simplifications. Both the analysis of the previous section and equation (5.4) suggest that for $f > 0.5$ the second-order equation

$$\bar{d}^2 - 2(C_V + C_\Upsilon - C_S)H^2 = 0 \tag{5.7}$$

can be used to obtain $\bar{d} = \sqrt{2(C_V + C_\Upsilon - C_S)}H$ which approximately ranges between $0.48H$ and $0.58H$ for $0.5 \leqslant f \leqslant 2$. Larger values of f would be too far outside the range considered in the computations and regressions would not be appropriate. However, all the evidence suggest that for $0 \leqslant f \leqslant 2$ we can assume $\bar{d} \approx H/2$ with good approximation.

In summary a simple 'recipe' is suggested to prescribe the SBCs. The motion of the mean shoreline is given by equation (4.1*a*) in which the rate of change of the volume in the swash zone, related to the local SW height through equation (5.1), acts to decelerate the shoreline motion during the runup and accelerate it during rundown. At the mean shoreline the mean water depth is computed to be about half of the local SW height.

If this is applied the following expressions can be used as a good approximation of

the SBCs for the wave-averaged water flows:

$$\frac{\mathrm{d}x_l}{\mathrm{d}t} \approx R_+ - \sqrt{2gH} - \frac{4C_V}{\alpha}\frac{\mathrm{d}H}{\mathrm{d}t}, \quad \bar{d}(x_l) \approx \frac{H}{2}, \quad \bar{u}(x_l) \approx R_+ - \sqrt{2gH}. \tag{5.8}$$

On the other hand, as suggested in Part 1, SW models may be chosen to permit the reflection of SW at x_l, i.e. by using relationships like those of equation (3.8).

Numerical investigation is currently underway to implement this 'recipe' in an available wave-averaged solver and preliminary results reveal that an accurate computation of R_+ at x_l is the most crucial issue for correctly predicting the motion of the mean shoreline. In order to confirm the validity of our analysis we are also planning to verify our findings on the basis of experimental evidence. At that stage it will also be necessary to take into account the different generation mechanisms (disregarded in the present analysis) of the shoreline low-frequency motion ('surf beat'). Preliminary analysis of new experimental data on surf beat generation by a time-varying breakpoint (Baldock *et al.* 2000) suggests our analysis is likely to be valuable for modelling those flow conditions: examples of experimental shoreline motion (e.g. figure 5*b* of Baldock *et al.* 2000) are surprisingly similar to our computed curves (e.g. figure 2).

Support from the European Union through the contract EVK3-2000-00037 (HUMOR) is acknowledged. Thanks are also due to the reviewers for their stimulating comments and for their suggestions which helped improve the clarity of presentation.

REFERENCES

Abramowitz, M. & Stegun, I. A. 1964 *Handbook of Mathematical Functions*. Dover.

Baldock, T. E., Huntley, D. A., Bird, P. A. D., O'Hare, T. J. & Bullock, G. N. 2000 Surf beat generation by a time-varying breakpoint. *Proc. 27th Intl Conf. Coastal Engng ASCE*, vol. 2, pp. 1398–1411.

Bellotti, G. & Brocchini, M. 2001 On the shoreline boundary conditions for Boussinesq-type models. *Intl J. Numer. Meth. Fluids* **37**, 479–500.

Brocchini, M. & Peregrine, D. H. 1996 Integral flow properties of the swash zone and averaging. *J. Fluid Mech.* **317**, 241–273.

Carrier, G. F. & Greenspan, H. P. 1958 Water waves of finite amplitude on a sloping beach. *J. Fluid Mech.* **4**, 97–109.

Guza, R. T. & Thornton, E. B. 1985 Observation of surf beat. *J. Geophys. Res.* **90**, 3161–3172.

Haas, K. A., Svendsen, I. A. & Haller, M. C. 1998 Numerical modelling of nearshore circulation on a barred beach with rip channels. *Proc. 26th Intl Conf. Coastal Engng ASCE*, vol. 1, pp. 801–814.

Kobayashi, N., Otta, A. K. & Roy, I. 1987 Wave reflection and run-up on rough slopes. *Proc. ASCE* **113**, 282–298.

Mei, C. C. 1989 *The Applied Dynamics of Ocean Surface Waves*. World Scientific.

Özkan-Haller, H. T. & Kirby, J. T. 1997 Nonlinear evolution of shear instabilities of the longshore current: A comparison of observations and computations. *J. Geophys. Res.* **104**, 25953–25984.

Peregrine, D. H. & Williams, S. M. 2001 Swash overtopping a truncated plane beach. *J. Fluid Mech.* **440**, 391–399.

Puleo, J. A. & Holland, K. T. 2001 Estimating swash zone friction coefficients on a sandy beach. *Coastal Engng* **43**, 25–40.

Shah, A. M. & Kamphuis, J. W.1996 The swash zone: a focus on low frequency motion. *Proc. 25th Intl Conf. Coastal Engng, ASCE*, vol. 2, pp. 1431–1442.

Van Dongeren, A. R. & Svendsen, I. A. 2000 Nonlinear and quasi 3-D effects in leaky infragravity waves. *Coastal Engng* **41**, 467–496.

Watson, G., Barnes, T. C. D. & Peregrine, D. H. 1994 The generation of low frequency waves by a single wave group incident on a beach. *Proc. 24th Intl Conf. on Coastal Engng, ASCE*, vol. 1, pp. 776–790.